Available online at www.sciencedirect.com
ScienceDirect
Journal of Molecular Catalysis A: Chemical 280 (2008) 43–51
JOURNAL OF MOLECULAR CATALYSIS A: CHEMICAL
www.elsevier.com/locate/molcata

Relationship between temperature-programmed reduction profile and activity of modified ferrite-based catalysts for WGS reaction

Ataullah Khan, Panagiotis G. Smirniotis *

Department of Chemical and Materials Engineering, University of Cincinnati, United States

Received 12 September 2007; accepted 14 October 2007
Available online 26 October 2007

Abstract

A series of modified ferrites were prepared by doping iron oxide with various transition/non-transition/inner-transition metal ions [M = Cr, Mn, Co, Ni, Cu, Zn and Ce] *in situ* during synthesis. All the modified ferrites thus obtained exhibit remarkably high surface areas, greater than that of pure iron oxide (Fe_2O_3) sample. The efficacy of the dopant ions in modifying the resultant specific surface area, could be directly related to variations in the rate of crystal growth. The nature and concentration of the foreign cations present in the system govern this variation. Interestingly all the modified ferrites, exhibit a narrow pore size distribution in the range of 4.9–25 nm. XRD analysis revealed the existence of hematite (Fe_2O_3) phase in all the as-prepared samples. The X-ray diffraction experiments performed on activated catalysts, confirmed the existence of magnetite (Fe_3O_4) phase with a nominal composition of $Fe_{2.73}M_{0.27}O_4$. These inverse or mixed spinels with general formula $A_{(1-\delta)}B_\delta[A_\delta B_{(2-\delta)}]O_4$, possess highly facile $Fe^{3+} \Leftrightarrow Fe^{2+}$ redox couple, the degree of facileness depends on the extent of synergistic interaction between iron and the other substitutent metal ion. The rapid electron hopping between $Fe^{3+} \Leftrightarrow Fe^{2+}$ in the Fe_3O_4 lattice system is essential to catalyze WGS reaction. From TPR it was observed that, incorporation of metal cations into the hematite (α-Fe_2O_3) crystal structure alters the reducibility of the hematite particles, which in turn depends on the nature of the incorporated metal cation. A plausible explanation for the WGS activity over various modified ferrites has been attempted with the help of TPR analysis.

Keywords: Modified ferrites; TPR; WGS reaction; Reducibility; Fe_3O_4; Fe_2O_3

1. Introduction

Spinel oxides are well known catalysts for various processes like oxidative dehydrogenation of hydrocarbons, decomposition of alcohols, selective oxidation of carbon monoxide, decomposition of hydrogen peroxide, and hydrodesulphurization [1–3]. Iron containing spinels are also called ferrospinels, and in ternary spinel systems Fe^{3+} ions can be easily shifted between octahedral (Oh) and tetrahedral (Td) sites by stoichiometrically varying the concentration of other substitutent cations. The catalytic properties of ferrospinels crucially depend on the nature of ions, their charges and their distribution among the Oh and Td sites of the spinel structure [4]. Substitution of 'Fe' centers in a ferrite with other transition/non-transition/inner-transition metals leads to the crystallization of an inverse or mixed spinel structure of composition $A_{(1-\delta)}B_\delta[A_\delta B_{(2-\delta)}]O_4$ where δ is the degree of inversion, while A and B represent typical cations possessing 2+ and 3+ charges on them, respectively. Such introduction is expected to strongly modify the redox properties of the resultant ferrites. Reithwisch and Dumesic studied a number of spinel structures (normal, mixed and inverse) and concluded that only inverse and mixed spinel structures can readily undergo rapid electron exchange between 2+ and 3+ ions, thereby catalyzing the WGS reaction [5]. The significant role of $Fe^{2+} \Leftrightarrow Fe^{3+}$ redox couple in WGS reaction was also demonstrated by Boreskov [6]. In magnetite-type (Fe_3O_4) of crystalline structures octahedral sites are occupied by 2+ and 3+ ions, while tetrahedral sites are occupied by 3+ ions only. The catalytic activity of spinels containing transition metal ions is influenced by the acid–base and redox properties of these ions as well as by their distribution among the octahedral and tetrahedral sites in the spinel structure. If one can facilitate tetrahedral sites to expand and octahedral sites to contract, an improvement in covalency of the system could result in promoting better electron hopping between these sites ($Fe^{2+} \Leftrightarrow Fe^{3+}$) and could result in better WGS activity [1,2].

* Corresponding author. Tel.: +1 513 556 1474; fax: +1 513 556 3473.
E-mail address: panagiotis.smirniotis@uc.edu (P.G. Smirniotis).

1381-1169/$ – see front matter © 2007 Elsevier B.V. All rights reserved.
doi:10.1016/j.molcata.2007.10.022

Iron exists in the form of three oxides, namely hematite (Fe_2O_3), magnetite (Fe_3O_4), and wustite (FeO). The latter is unstable below 570 °C, where it decomposes to α-Fe and Fe_3O_4 [7]. As per literature the reduction of Fe_2O_3 to Fe metal, at temperatures below 570 °C, proceeds in two steps via Fe_3O_4 intermediate. The $Fe_2O_3 \rightarrow Fe_3O_4$ reduction is exothermic, while reduction to the metal is endothermic [8]. Depending on the type of sample, experimental conditions employed, variations in the TPR profile can be observed. In particular, differences are found in the literature in the conditions of reduction temperature, H_2O partial pressure, and particle size. Addition of a dopant material significantly modifies the reduction behavior of the samples. The aim of the present study is to clarify, by means of temperature-programmed reduction (TPR), the effect of dopant on the reducibility of iron oxide-based WGS catalysts prepared by an analogous route. The information obtained from TPR will be utilized to get better understanding of the resultant WGS activity.

2. Experimental

2.1. Preparation of modified ferrites

Selected metal doped iron oxide-based catalysts with nominal composition of $Fe_{1.82}M_{0.18}O_3$ [where M = Cr, Mn, Co, Ni, Cu, Zn, and Ce] were prepared in 10:1 (Fe:M) atomic ratio by co-precipitation route. Nitrate precursors were employed for all the preparations. In a typical preparation, calculated amounts of iron nitrates and other metal nitrate were dissolved separately in deionized water and mixed together. Dilute aqueous ammonia was added gradually dropwise to the aforementioned mixture solutions, with vigorous stirring, until precipitation was complete (pH 8.5). The supernatant was analyzed for nitrate ions by adding about 1 ml concentrated sulphuric acid to 10 ml of the supernatant, the formation of $[Fe(NO)]^{2+}$ can be detected by a brown ring [9]. The non-formation of brown ring was observed in all the cases. Thus, the obtained precipitate gels were further aged overnight, and filtered off. The obtained cakes were oven dried at 80 °C for 12 h and finally calcined at 500 °C for 3 h in inert environment. The rate of heating as well as cooling was always maintained at 5 °C min^{-1}. The precipitation process is dictated by solution thermodynamics. The solution reaches saturation state when the dissolution rate equals the precipitation rate. Nucleation starts when the solution concentration exceeds the saturation concentration. The solution concentration affects the crystallite size of the precipitated catalyst. In the present investigation, the concentration of the nitrate solution was optimized so as yield nanosized grains. It is notable that all catalysts reported here are prepared by completely analogous procedures, which is necessary to allow direct comparison of their catalytic properties.

2.2. Preparation of pristine oxides

The pristine oxides of Cr, Mn, Fe, Co, Ni, Cu, Zn and Ce were prepared by an analogous soft solution chemical route, as described in the above paragraph. Corresponding nitrate salt precursor was dissolved in deionized water and titrated with

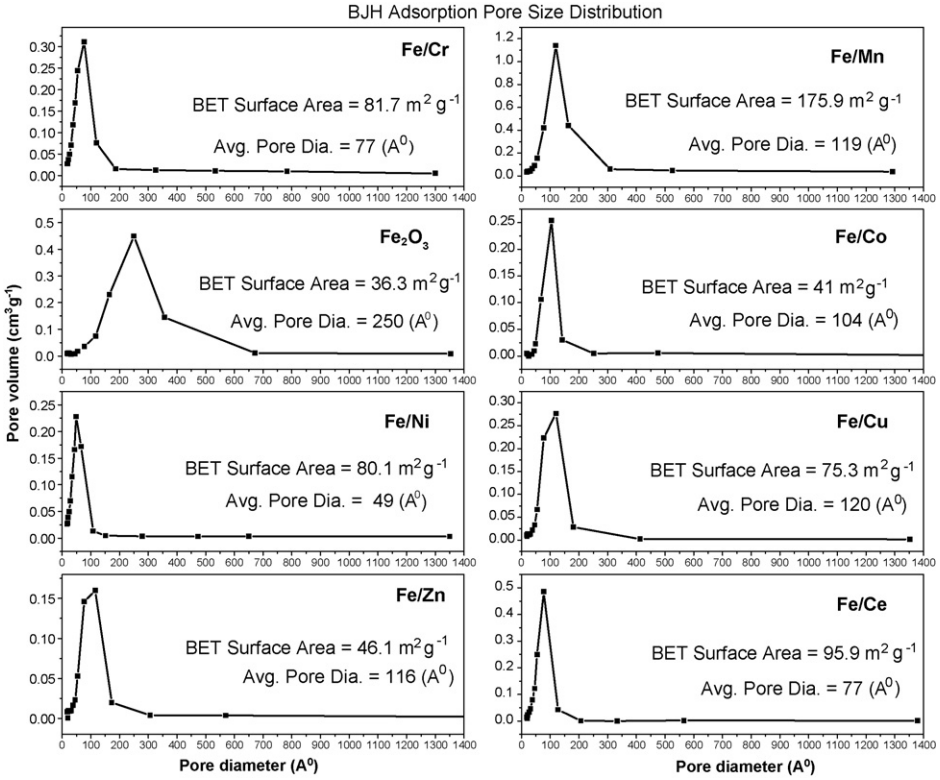

Fig. 1. Pore size distribution (PSD) plots of various modified ferrites Fe/M [10:1] (M = Cr, Mn, Co, Ni, Cu, Zn and Ce).

dilute aqueous ammonia until precipitation was complete (pH 8.5). The dried hydroxide gel was calcined at 500 °C for 3 h in inert environment.

2.3. Catalyst characterization

2.3.1. Surface area and pore size distribution analysis

The BET surface areas were obtained by N_2 adsorption on a Micromeritics Gemini 2360 Instrument. Prior to analysis, samples were oven dried at 120 °C for 12 h and flushed with Argon for 2 h. The pore size distribution analyses were conducted by N_2 physisorption at liquid N_2 temperature using Micromeritics ASAP 2010 apparatus. All samples were degassed at 300 °C under vacuum before analysis.

2.3.2. X-ray diffraction measurements

Powder X-ray diffraction (XRD) patterns were recorded on a Phillips Xpert diffractometer using nickel-filtered Cu Kα (0.154056 nm) radiation source. The intensity data were collected over a 2θ range of 3–80° with a 0.02° step size and using a counting time of 1 s per point. Crystalline phases were identified by comparison with the reference data from ICDD files [10].

2.3.3. TPR measurements

The temperature-programmed reduction (TPR) with hydrogen, of various catalyst samples were performed by means of an automated catalyst characterization system (Micromeritics, model AutoChem II 2920), which incorporates a thermal conductivity detector (TCD). The experiments were carried out at a heating rate of 5 °C/min. The reactive gas composition was H_2 (10 vol.%) in Argon. The flow rate was fixed at 10 ml/min (STP). The total reactive gas consumption during TPR analysis was measured. The TPR measurements were carried out following activation after cooling the sample in helium flow to 50 °C. The sample was then held at 50 °C under flowing helium to remove the remaining adsorbed oxygen until the TCD signal returned to the baseline. Subsequently the TPR experiments were performed up to a temperature 800 °C or 1000 °C.

2.4. Catalyst activity

The WGS reaction was carried out in a vertical down flow fixed bed differential ceramic microreactor (i.d. 0.635 cm) at atmospheric pressure. In a typical experiment, ca. 0.1 g of sieved catalyst was placed between two plugs of quartz wool. The reactor was placed vertically inside a programmable tubular furnace (Lindberg), which was heated electrically. Prior to the reaction, the catalyst was pre-treated in flowing process gas at 400 °C for 4 h. The catalyst pretreatment involves the partial reduction of hematite (Fe_2O_3) to magnetite (Fe_3O_4) using a mixture of H_2, CO, CO_2 (99.9% pure gases) and water vapor [11–13]. It is important to avoid over-reduction of the magnetite

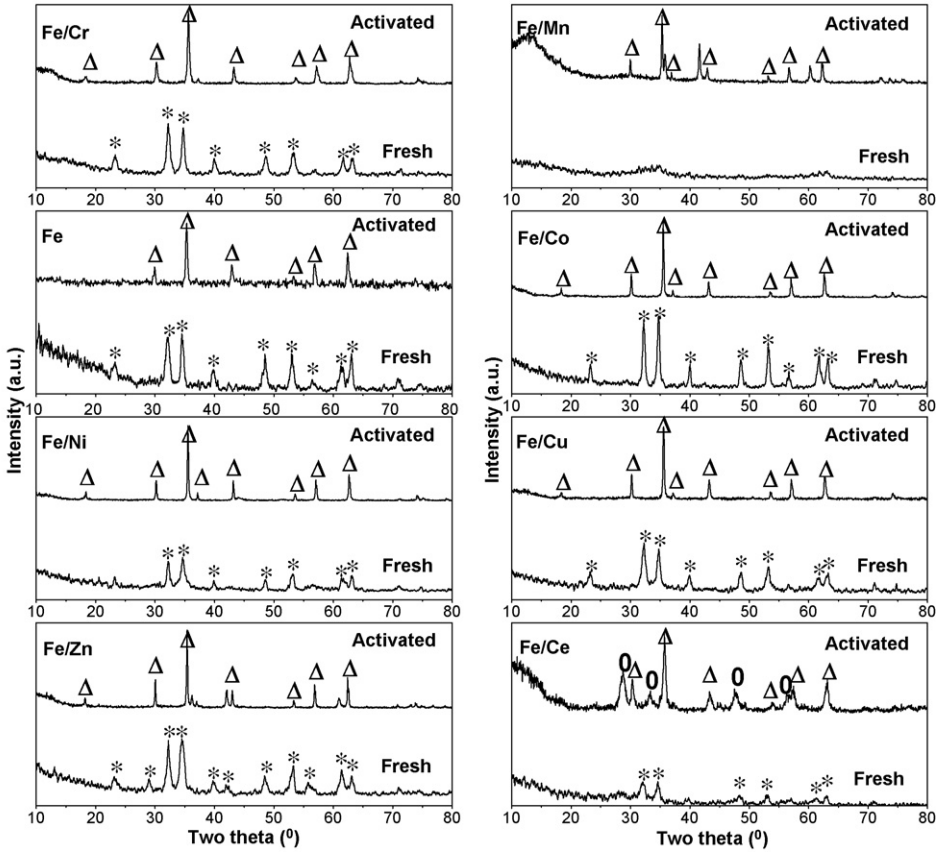

Fig. 2. X-ray powder diffraction patterns of various as-prepared and activated modified ferrites Fe/M [10:1] (M = Cr, Mn, Co, Ni, Cu, Zn and Ce). (*) lines due to Fe_2O_3; (△) lines due to Fe_3O_4; (0) lines due to CeO_2.

active phase to lower carbides, oxides or metallic iron phases. Metallic iron phases are active catalysts for methanation and Fischer–Tropsch processes [11]. The rate of heating and cooling was always maintained at 5 °C min^{-1}. The gas flows were regulated through pre-calibrated mass flow controllers with digital read-out unit (MKS instruments). Water was injected into the system through a motorized syringe pump (Cole-Parmer type 74900) to generate steam. The entire system was kept at 200 °C by using heating tapes. Before pre-treatment the reactor set-up was flushed with an inert gas, the pre-treatment gas mixture was initialized only after the catalytic system had attained temperatures higher that 150 °C. The experiments were performed in the temperature range of 350–550 °C using a designated amount of steam and CO. The product stream coming from the reactor was passed through ice cooled trap to condense water, after which, the product gases were analyzed with an on-line TCD (Gow Mac series 550 thermal conductivity detector) having a porapak Q column for separation of the gases. This TCD was interfaced to a personal computer using a peak simple chromatography data system. The post analyses of results were done on the peak simple 2.31 software. The product-gas was injected through a six port valve, sampling was performed at every 20 min interval. Reported values of conversions correspond to steady-state values (0.5 h). The gas hourly space velocity of 60,000 h^{-1} was maintained in the experiments. A steam/dry gas ratio of 3.5, was employed in the present investigation.

3. Results and discussion

The BET surface area and pore size distribution analyses was performed on various metal incorporated iron oxides of composition $Fe_{1.82}M_{0.18}O_3$ (M = Cr, Mn, Co, Ni, Cu, Zn and Ce) the corresponding results are shown in Fig. 1. In general, ferrites substituted with different transition/non-transition/inner-transition metal ions exhibit variable surface areas; the variation in turn depends on the selection of substitutent metal ion. The efficacy of the substitutent cations in modifying the resultant specific surface area could be directly related to variations in the rate of crystal growth. The nature and concentration of the foreign cations present in the system govern this variation. Among all the catalysts investigated in this report, Fe/Mn exhibits the maximum surface area, while the lowest surface area was displayed by Fe/Co sample. A narrow pore size distribution in the range of 4.9–25 nm was observed for all the investigated samples.

In order to ascertain the composition and phase purity, XRD examination was performed on the various modified ferrites in both as-prepared and activated forms as shown in Fig. 2. Interestingly, all the as-prepared modified ferrite samples (except Fe/Mn and Fe/Ce) exhibit intense and similar type of XRD patterns. Existence of Fe_2O_3 type phase (PDF-ICDD 33-0664) was identified by comparison with standard reference data from PDF data base. Additionally, the XRD spectra for the modified ferrite samples do not show any extra crystalline phases due to individual oxides of the substitutent cations, such as MO_x [M = Cr, Mn, Co, Ni, Cu, Zn and Ce]. The XRD analyses performed on the activated catalysts revealed the existence of Fe_3O_4 (magnetite) type diffraction patterns (PDF-ICDD 26-1136). In the case of activated Fe/Ce, along with Fe_3O_4, presence of CeO_2 crystalline phase (PDF-ICDD 34-0394) could be noted.

Before performing the WGS reaction, the as prepared catalysts which are in hematitic form have to be activated to magnetite form by controlled reduction in a stream of CO, CO_2, H_2, and H_2O vapor. The over-reduction leads to the formation of FeO, Fe_2C and metallic iron phases, which catalyze undesired side reactions like methanation and CO disproportionation [14]. The results of the experiments carried out at different temperatures, over various activated modified ferrite-based shift catalysts are shown in Fig. 3. A solid line in Fig. 3 represents the variation of the thermodynamic equilibrium CO conversion as a function of temperature. As inferred from the solid line, the equilibrium conversion of CO decreases with raise in the reaction temperature, as WGS reaction is a moderately exothermic. It is observed from Fig. 3, that the WGS activity over various activated modified ferrites increases with the temperature, due to kinetic factors [15]. It is suggested that at lower temperatures (350 °C) the activity of magnetite is limited by the dissociation of steam over its surface [16].

The reductions of Fe_2O_3 and Fe_3O_4 to Fe have been reported to follow either of three models, namely nucleation, autocatalytic, or contracting sphere (phase boundary) models of reduction, with variations attributed to experimental factors such

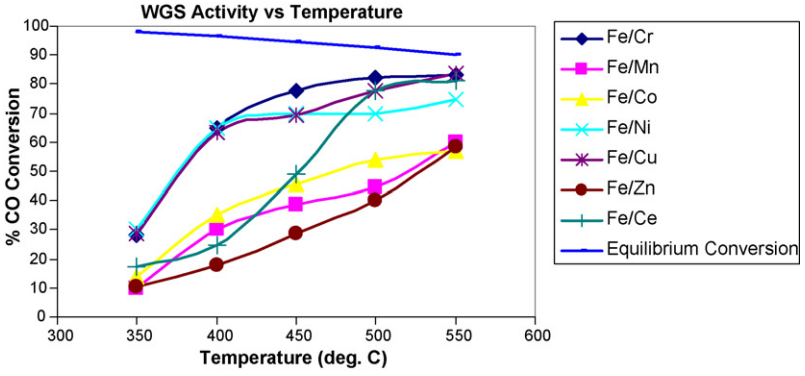

Fig. 3. The WGS activity results over various activated modified ferrites Fe/M [10:1] (M = Cr, Mn, Co, Ni, Cu, Zn and Ce) in the temperature range 350–550 °C; steam/CO = 3.5; gas hourly space velocity (GHSV) = 60,000 h^{-1}; a solid line (in blue) represents the variation of the thermodynamic equilibrium conversion of CO (%) as a function of temperature.

as sample particle size or the conditions chosen for analysis [17,18]. Larger particle sizes have been reported to reduce via a phase boundary mechanism (topochemical mode of reaction) while smaller particles tend to show sigmoidal reduction isotherms associated with a formation and growth of nuclei model (uniform internal reduction) [17–19]. In the case of reduction of either hematite or magnetite at temperatures above 600 °C, the formation of a stable wustite phase must also be considered. In the reported TPR of pure hematite (Fe_2O_3), the first reduction peak appears at 302 °C, corresponding to the transition of Fe_2O_3 to Fe_3O_4. The second peak at 354 °C was attributed to the transformation of Fe_3O_4 to FeO. The third and final peak at 475 °C corresponds to the transition of FeO to Fe [20]. In another report, the TPR curves of hematite showed a peak at 510 °C, assigned to magnetite formation, and another around 770 °C, attributed to the formation of metallic iron [21]. The position of the temperature maxima may vary from sample to sample depending on the particle size and other parameters such as temperature ramp rate. Addition of a substitutent/dopant ion significantly modifies the reduction profile, as compared to that of the pristine Fe_2O_3 sample [8].

The TPR profiles of the various metal-doped iron oxide-based catalysts are presented in Fig. 4. For the purpose of reference the TPR profile of pristine Fe_2O_3 (free from any substitutent ion) prepared by similar procedure, is included in Fig. 4A. In the TPR of pristine hematite (Fe_2O_3), the first reduction peak appears at 348 °C, corresponding to the reductive transition of Fe_2O_3 to Fe_3O_4. The peak at 621 °C corresponds to the transformation of Fe_3O_4 to FeO. Under the experimental conditions of the present study, complete reduction of FeO to metallic Fe was not observed even up to 800 °C, only partial reduction took place. From Fig. 4B–H, it is obvious that, each promoter [M = Cr, Mn, Co, Ni, Cu, Zn, and Ce] influences the reduction profile of iron oxide in a very unique manner. Therefore, in order to better understand the specific role of each promoter on the reducibility of hematite phase, TPR studies were conducted on each individual pristine oxide MOx [M = Cr, Mn, Co, Ni, Cu, Zn, and Ce], the corresponding TPR profiles are shown in Fig. 5. From Fig. 5, it can be noted that, in case of pristine CrO_x only one reductive transition from Cr^{6+} to Cr^{3+} was observed at 311 °C, beyond which no H_2 consumption could be noted even up to 1000 °C. the TPR profile of pristine MnO_x exhibits two well defined H_2-TPR peaks; the first peak observed at 292 °C T_{max} can be attributed to the $MnO_2 \rightarrow Mn_2O_3$ reductive transition, while the 440 °C T_{max} peak is representative of the $Mn_2O_3 \rightarrow MnO$ reduction. Pristine CoO_x is composed of two distinct reductive transitions, namely

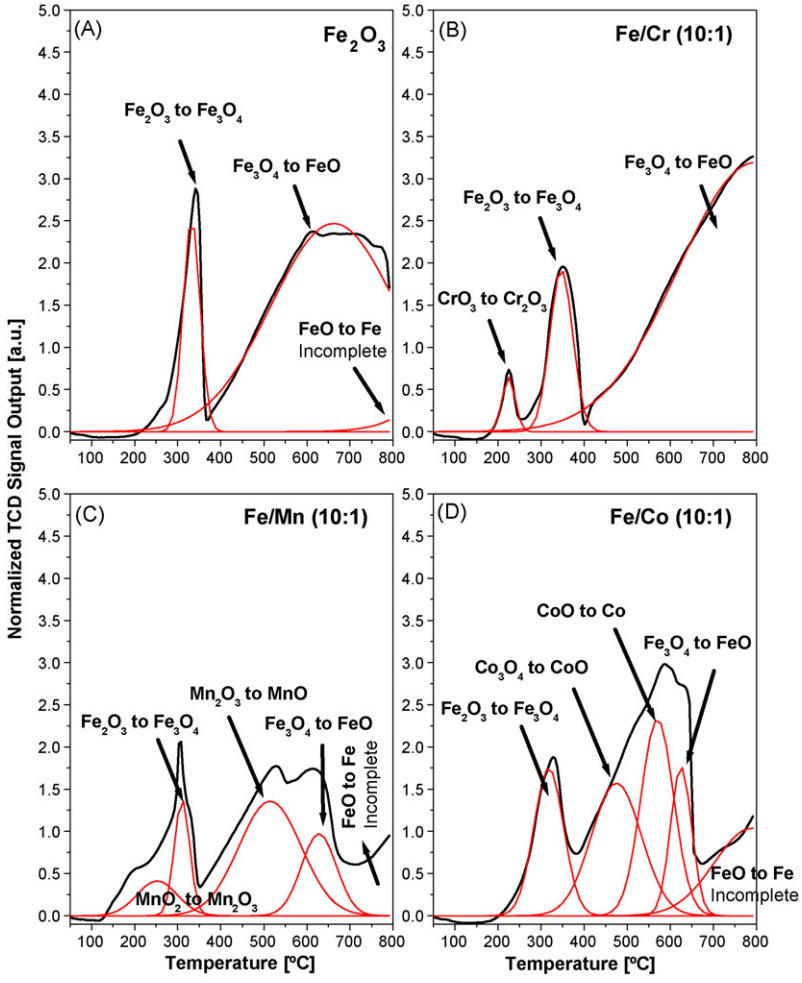

Fig. 4. TPR profiles of various modified ferrites Fe/M [10:1] (M = Cr, Mn, Co, Ni, Cu, Zn and Ce).

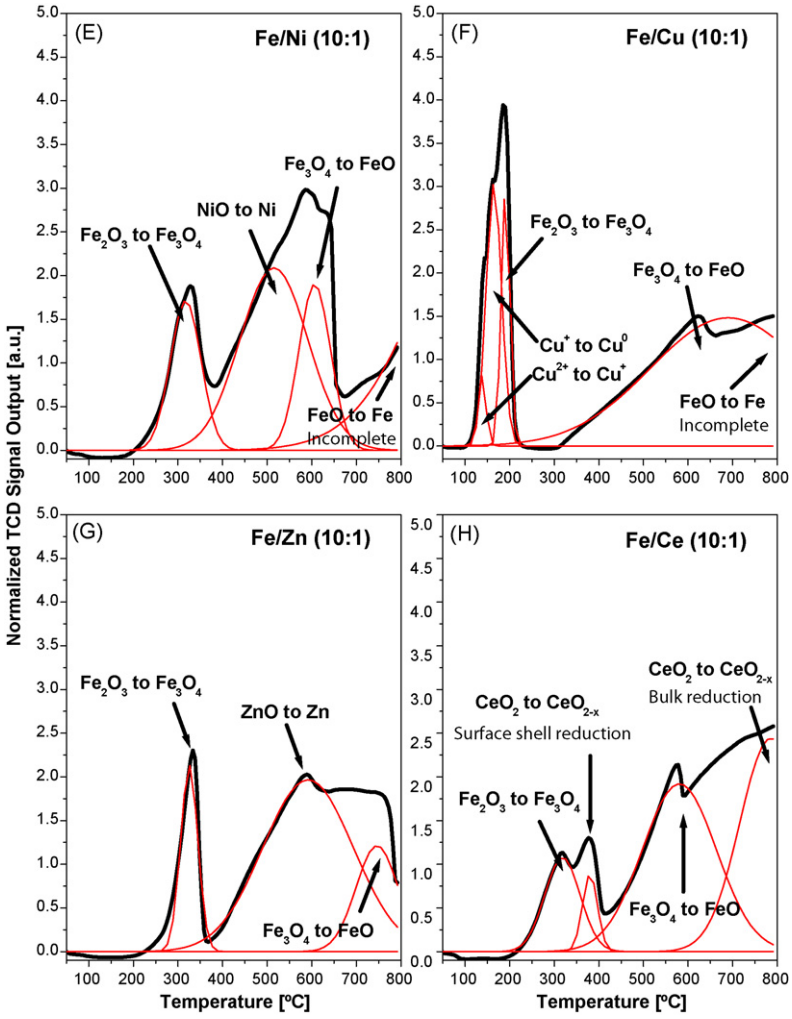

Fig. 4. (*Continued*).

Co_3O_4 to CoO and CoO to Co observed at T_{max} 332 °C and 350–600 °C, respectively. In the case of pristine NiO_x and CuO_x samples, only single stage H_2 consumption could be observed, which is representative of the formation of metallic Ni/Cu. Two distinct H_2-consumption peaks were noted (at 465 and 800 °C) in the TPR profile of pristine ZnO, which could be attributed to the reduction of Zn^{2+} to Zn^0 and sublimation, respectively [22,23]. In the TPR of pristine CeO_2, two reduction peaks were observed, at 485 °C and beyond 800 °C, which can be respectively, attributed to the existence of two types of oxygen anions in CeO_2: surface oxygens situated in a tetrahedral coordination site bound to one Ce^{4+} ion and bulk oxygens bound to Ce^{4+} [24,25].

In the case of Fe/Cr catalyst, the first reduction peak at 225 °C corresponds to the reduction of $Cr^{6+} \rightarrow Cr^{3+}$ (Fig. 4B), interestingly further partial reduction of $Cr^{3+} \rightarrow Cr^{2+}$, which is well-documented in literature [26] was not observed in the present study. Reduction of $Fe_2O_3 \rightarrow Fe_3O_4$ was observed at 350 °C T_{max}, while further reduction to FeO occurs at higher temperatures. Addition of chromium to Fe_2O_3, did not improve the reducibility of hematite → magnetite. Coming to Fe/Mn catalyst, the first reduction peak at 200 °C corresponds to reduction of $Mn^{4+} \rightarrow Mn^{3+}$, while the reduction of $Mn^{3+} \rightarrow Mn^{2+}$ occurs at 528 °C (Fig. 4C). In particular, Fe/Mn system presents a typical example of cooperative synergistic influence (synergism) of both Mn and Fe on each other's reduction profiles. An important feature observed in the TPR profile of Fe/Mn is a shift of the iron oxide TPR peaks to lower temperatures (by ∼50 °C), inferring that the presence of Mn facilitates the reduction of Fe^{3+} species [Fe_2O_3 to Fe_3O_4]. The 613 °C T_{max} peak corresponds to the reduction of magnetite to wustite, beyond which total reduction to metallic iron is expected to occur. The reduction profile for pristine Co_3O_4 comprises of a low-temperature peak below ∼300 °C or ∼330 °C (Fig. 5) and a high-temperature peak between 350 and 600 °C (Fig. 5) or as reported by Brown et al., between 300 and 700 °C, which correspond to the following processes, respectively, $Co_3O_4 \rightarrow CoO \rightarrow Co$ [27]. Addition of cobalt to iron oxide, causes the temperature of the maximum rate of hydrogen uptake [for $Fe_2O_3 \rightarrow Fe_3O_4$] to be lower by 20 °C (from 350 to 330 °C) indicating that the presence of cobalt makes the hematite easier to reduce (Fig. 4D). The observed TPR pattern matches well with the literature reports on iron–cobalt

catalysts [27]. In the TPR profile of Fe/Ni (Fig. 4E), the reduction of hematite to magnetite is observed at 327 °C, followed by the reduction of Ni^{2+} to Ni^0 at ~510 °C, and finally magnetite to wustite reductive transition was observed at 590 °C. Even up to 800 °C, formation of metallic iron could not be observed. In the case of Fe/Cu catalyst (Fig. 4F) the first peak at 143 °C corresponds to reduction of $Cu^{2+} \rightarrow Cu^{+}$, and the subsequent peak at 162 °C is due to reduction of $Cu^{+} \rightarrow Cu^{0}$. In general the resolution of Cu reduction peaks is very poor and its very difficult to designate each stage of reduction, however in the present study, Fe/Cu reduction profile gave well resolved peaks for each step of copper reduction i.e., +2 to +1 and +1 to 0. The temperature maxima thus obtained agree well with the values previously reported in the literature [28]. Interesting observation from the present study is that addition of Cu to Fe_2O_3, considerably brought down the reduction temperature of hematite to magnetite to 190 °C as compared to 348 °C which is observed in pristine hematite sample. It is well know that presence of even 1 at.% Cu shifts the peak reduction temperature by >100 °C [29]. Interestingly, addition of Cu did not affect the stability of Fe_3O_4 phase, which was found to be stable up to 600 °C, thats where transformation of the magnetite to wustite was observed in the present study. The TPR profile (Fig. 4G) of Fe/Zn catalyst is very similar to that of the pristine Fe_2O_3 sample. The peak at 333 °C can be attributed to the formation of magnetite phase, while reduction of Zn^{2+} to Zn^0 was observed at ~588 °C, beyond which formation of wustite phase was noted. In the TPR of pristine-ZnO, the reduction of Zn^{2+} to Zn^0 is observed at 465 °C, while sublimation is observed above 800 °C. As per literature reports the region of [22,23] Zn sublimation and desorption occurs at around 600 °C, which can be substantially lower under severe reductive atmosphere or vacuum [30,31]. The enhanced reducibility observed in the case of Fe/Ce catalyst (Fig. 4H), can be related to the close interaction between Fe and Ce cations, which occurs during co-precipitation process. Pristine ceria shows two characteristic reduction regimes, surface shell reduction (485 °C) and bulk reduction (850 °C). Upon promoting iron oxide with cerium causes the reduction peaks of

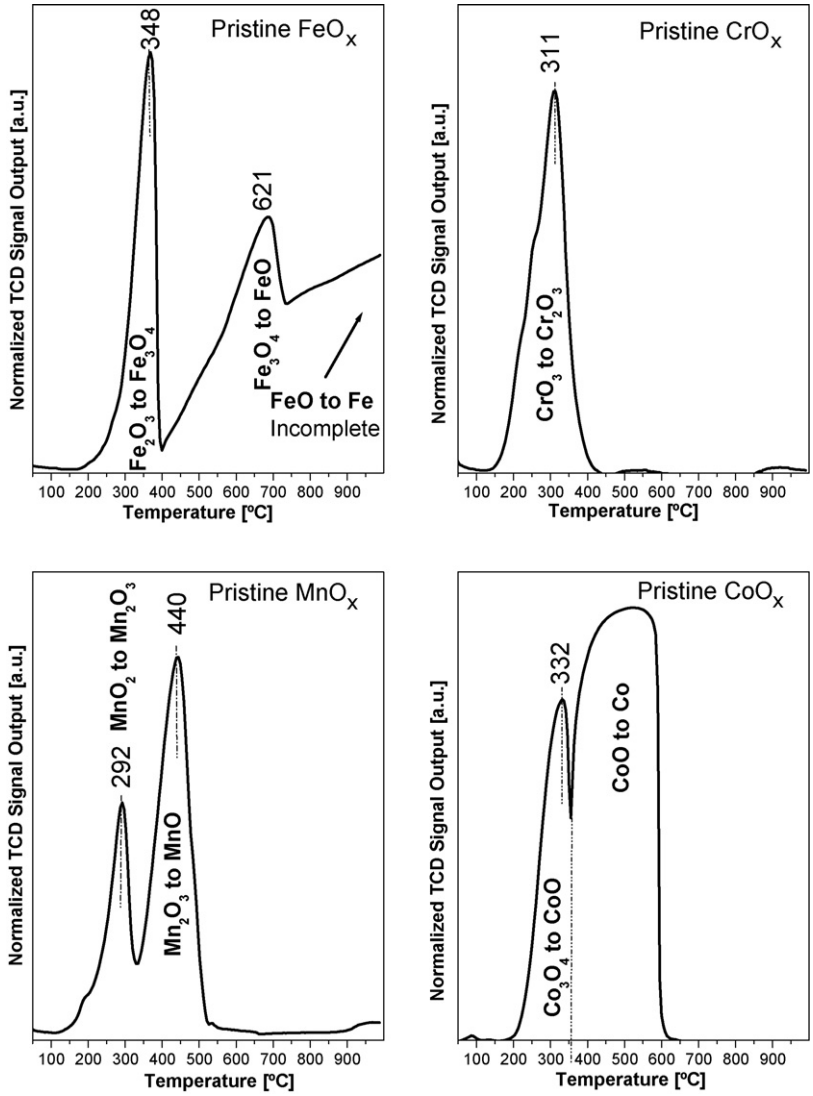

Fig. 5. TPR profiles of various pristine MO_x (M = Cr, Mn, Fe, Co, Ni, Cu, Zn and Ce) oxide samples.

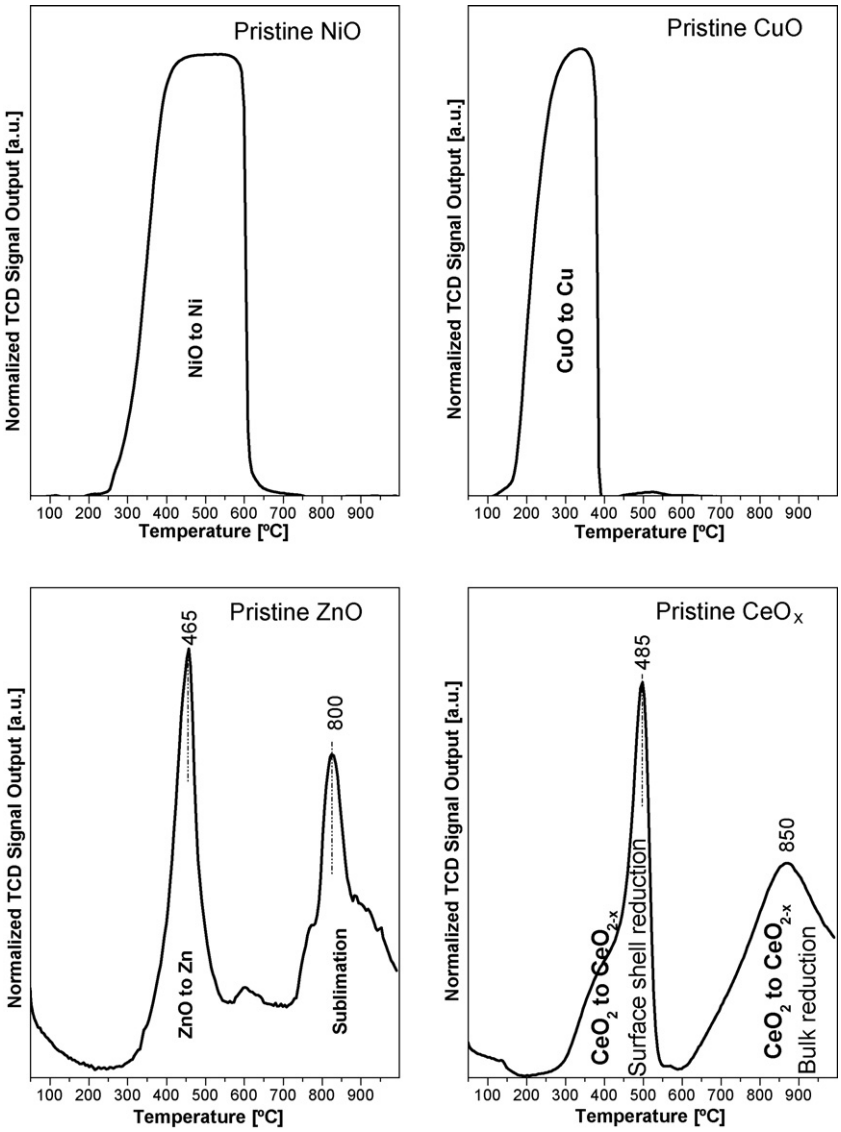

Fig. 5. (*Continued*).

both hematite-to-magnetite and magnetite-to-wustite to shift to lower temperatures. The ceria surface shell reduction in the case of Fe/Ce system occurs at 380 °C, instead of 485 °C as in the pristine ceria sample, however the ceria bulk reduction is not affected by the presence of iron. According to Trovarelli and co-workers [24] TPR trace for ceria is not controlled by the rate of diffusion of the oxygen vacancies, instead surface reduction process and the difference of both thermodynamic and kinetic properties existing in the ceria micro-crystals (as a function of their size) are critical factors. Within the experimental conditions of the present study formation of metallic iron species was either delayed (prolonged) or not observed, which can be attributed to the method of preparation employed in this investigation. On the whole, promoting iron oxide with Cu, improved the reducibility of hematite to greater extent. Similarly promotion was observed when substitutent ions like Mn, Co, Ni, Zn and Ce were incorporated in to the iron oxide crystal lattice. The WGS reaction is a redox process, wherein facile reducibility of Fe^{3+} species enhances the WGS activity.

3.1. Structure activity relationship

From our studies, it is observed that simultaneous precipitation of substitutent metal cation (M^{n+}) with Fe^{3+} leads to the formation of hematitic type $Fe_{1.82}M_{0.18}O_3$ phase, which upon activation transforms into either inverse or mixed $Fe_{2.73}M_{0.27}O_4$ spinel. The overall WGS activity depends on various parameters like operation conditions, nature of substitutent ion incorporated, and covalency of the $Fe^{III} \leftrightarrow Fe^{II}$ redox couple in the resultant catalyst. Topsoe and Boudart [32] found that expansion of tetrahedral sites and contraction of octahedral sites leads to increased covalency in the system and improved electron hopping capabilities between $Fe^{III} \leftrightarrow Fe^{II}$ octahedral sites. Moreover, improving the covalency of the catalysts, improves the WGS activity [6]. Boreskov has demonstrated that the octahedral Fe^{2+} and Fe^{3+} ions located in octahedral sites in the magnetite-based structure function as a redox couple, and magnetite based catalysts can be highly effective for the complete dissociation of water into hydrogen and adsorbed oxygen under

reaction conditions. Water dissociation causes the oxidation of Fe^{2+} centers to Fe^{3+} and liberates hydrogen. The oxidized iron centers may subsequently be reduced by CO thereby producing CO_2 to complete the reaction loop [6]. Cr_2O_3 is a well known refractory oxide. The presence of chromium, restricts the rapid thermal sintering of Fe_3O_4, thereby enhances the WGS activity of the Fe/Cr catalyst. It is proposed that iron–chromia form inverse spinel and that Cr^{3+} replaces equal amounts of Fe^{2+} and Fe^{3+} from the octahedral sites and the displaced Fe^{2+} were consequently located in tetrahedral site [32]. Addition of Cu to iron oxide results in improved reducibility of Fe^{3+} species into Fe^{2+}, thereby promoting the WGS activity. Also it is well known that doping with Cu increases the mobility of lattice oxygen and hydroxyl groups, on account of increased electronegativity in Fe/Cu compared to the pristine Fe_3O_4 sample, there by results in better catalytic activity [33]. Iron–ceria-based WGS catalysts are promising because of the oxygen storage capacity (OSC) of ceria and the co-operative effect between cerium and iron oxides. Interestingly, both iron and ceria possess highly facile $Fe^{III} \leftrightarrow Fe^{II}$ and $Ce^{IV} \leftrightarrow Ce^{III}$ redox couples, respectively; the synergism between the two couple could be responsible for the improved WGS activity. Additionally, the increase in WGS activity with increase in temperature could be due to the improvement in the OSC of ceria [34]. The synergistic effect could be primarily attributed to the formation of either inverse or mixed spinels of composition $A_{(1-\delta)}B_{\delta}[A_{\delta}B_{(2-\delta)}]O_4$ which possess highly facile $Fe^{3+} \Leftrightarrow Fe^{2+}$ redox couple. The resultant WGS activity can be related to the degree of covalency ($Fe^{3+} \Leftrightarrow Fe^{2+}$ redox couple), which in turn depends on the ease of reducibility, operation conditions and catalyst formulation.

4. Conclusions

Simultaneous precipitation of Fe(III) nitrates along with substitutent metal nitrate (of Cr, Mn, Co, Ni, Cu, Zn or Ce), results in the formation of nanocrystalline, high surface area ferrites. XRD data analyses of activated catalysts established the existence of $Fe_{2.73}M_{0.27}O_4$ (M = Cr, Mn, Co, Ni, Cu, Zn and Ce) type inverse and mixed spinels. These $A_{(1-\delta)}B_{\delta}[A_{\delta}B_{(2-\delta)}]O_4$ spinels (inverse or mixed), possess highly facile $Fe^{3+} \Leftrightarrow Fe^{2+}$ redox couple, the degree of facileness depends on the extent of synergistic interaction between iron and the other substitutent metal ion. From TPR it was observed that, incorporation of metal cations into the hematite (α-Fe_2O_3) crystal structure alters the reducibility of the hematite particles, which in turn depends on the nature of the incorporated metal cation. The resultant WGS activity can be related to the degree of covalency ($Fe^{3+} \Leftrightarrow Fe^{2+}$ redox couple), which in turn depends on the ease of reducibility, operation conditions and catalyst formulation.

Acknowledgment

Financial support was provided by the U.S. Department of Energy (grant DE-PS36-03GO93007).

References

[1] R.J. Rennard, W.L. Khel, US Patents 34,507,886 and 34,507,887 (1969).
[2] P.N. Rylander, W.J. Zimmerschied, US Patent 2,805,187 (1957).
[3] I. Keizoo, T. Toshio, K. Maso, A. Toshikazu, Jpn. Kokai Tokkyo Koho 74 (1976) 102590;
I. Keizoo, T. Toshio, K. Maso, A. Toshikazu, Jpn. Kokai Tokkyo Koho 75 (1976) 123174;
I. Keizoo, T. Toshio, K. Maso, A. Toshikazu, Jpn. Kokai Tokkyo Koho 74 (1976) 120886.
[4] R.J. Rennard, W.L. Kehl, J. Catal. 21 (1971) 282.
[5] D.G. Reithwisch, J.A. Dumesic, Appl. Catal. 97 (1986) 109.
[6] G.K. Boreskov, Kinet. Katal. 11 (1970) 374.
[7] J.O. Edstrom, J. Iron Steel Inst. 175 (1953) 289.
[8] M.V.C. Sastri, R.P. Vishwanath, B. Vishwanath, Int. J. Hydrogen Energy 7 (1982) 951.
[9] G.C. Araujo, M.C. Rangel, Catal. Today 62 (2000) 201.
[10] H.P. Klug, L.E. Alexander, X-ray Diffraction Procedures for Polycrystalline and Amorphous Materials, 2nd ed., Wiley, New York, 1974.
[11] C. Rhodes, G.J. Hutchings, A.M. Ward, Catal. Today 23 (1995) 43.
[12] C. Rhodes, B.P. Williams, F. King, G.J. Hutchings, Catal. Commun. 3 (2002) 381.
[13] E. Xue, M. O'Keeffe, J.R.H. Ross, Catal. Today 30 (1996) 107.
[14] M.V. Twigg, Catalyst Handbook, 2nd ed., Wolfe Publishing, London, 1989, p. 268–288.
[15] D.S. Newsome, Catal. Rev. Sci. Eng. 21 (1980) 275.
[16] E.F. Armstrong, T.P. Hilditch, Proc. Roy. Soc. A97 (1920) 265.
[17] O.J. Wimmers, P. Arnoldy, J.A. Moulijn, J. Phys. Chem. 90 (1986) 1331.
[18] H. Jung, W. Thompson, J. Catal. 128 (1991) 218.
[19] D.A. Monti, A. Baiker, J. Catal. 83 (1983) 323.
[20] P.A. Webb, MIC Technical Publications, January 2003, pp. 1–12.
[21] J.C. Gonzalez, M.G. Gonzalez, M.A. Laborde, N. Moreno, Appl. Catal. 20 (1986) 3.
[22] O.W. P-Lopez, A.C. Farias, N.R. Marcilio, J.M.C. Bueno, Mater. Res. Bull. 40 (2005) 2089.
[23] J.M.C. Bueno, M. Gazzano, M.G. Coelho, A. Vacari, Appl. Catal. A 103 (1993) 69.
[24] F. Giordano, A. Trovarelli, C. de Leitenburg, M. Giona, J. Catal. 193 (2000) 273.
[25] H.C. Yao, Y.F. Yu Yao, J. Catal. 86 (1984) 254.
[26] E.P. Reddy, B. Sun, P.G. Panagiotis, J. Phys. Chem. B 108 (2004) 17198.
[27] R. Brown, M.E. Cooper, D.A. Whan, Appl. Catal. 3 (1982) 177.
[28] J.Y. Kim, J.A. Rodriguez, J.C. Hanson, A.I. Frenkel, P.L. Lee, J. Am. Chem. Soc. 123 (2003) 10684.
[29] G.C. de Araujo, M. do, C. Rangel, Catal. Today 62 (2000) 201.
[30] W. Makwa, D. Kohl, G. Heiland, Surf. Sci. 99 (1980) 202.
[31] K. Lui, M. Vest, P. Berlowitz, S. Akhter, H.H. Kung, J. Phys. Chem. 90 (1986) 3183.
[32] H. Topsoe, M. Boudart, J. Catal. 31 (1973) 346.
[33] W.F. Podolski, Y.G. Kim, Ind. Eng. Chem. Process Des. Dev. 13 (1974) 415.
[34] F.J. P-Alonso, I. M-Cabrera, M.L. Granados, F. Kapteijn, J.L.G. Fierro, J. Catal. 239 (2006) 340.